

Fast Inverse Perspective Mapping and its Applications to Road State Detection

Gang Yi JIANG, Jae Won Eom, Byung Suk Song*, Jae Wook Bae*,
Tae Young CHOI, Suk Kyo HONG

Division of Electronics Engineering, Ajou University, *Institute of Advanced Engineering
5 Wonchong-dong, Paldal-ku, Suwon-city, 442-749, KOREA

*YoongIn P.O. Box 25, Kyonggi-Do, 449-020, KOREA

Tel: +82-331-219-2362, Fax: +82-331-212-9531

E-mail: taeyoung@madang.ajou.ac.kr

Abstract: An improved inverse perspective mapping (IIPM) is proposed so as to reduce computational expense of recovery of 3D road surface. An experimental system based on IIPM is developed to detect lane parameters for a driver assistant system. A re-organized image is obtained quickly and exactly by IIPM. Efficient preprocessing techniques are used to enhance the information of lane and obstacles. Lane in the preprocessed image is located with region identification. Lane parameters are estimated effectively. An algorithm to adaptively modify the parameters of IIPM is given. Properties of obstacle on 3D road surface are discussed and used to detect obstacles in the current lane and neighboring lanes. Experimental results show that the new method can extract lane state information effectively.

1. Introduction

Numerous accidents are caused by driver inattention or driver impairment. To reduce the occurrence of such accidents, driver assistance systems are designed to warn drivers and to help them to keep their vehicles in their proper lane and away from obstacles. The key function of a driver assistance system is automatic detection of the lane and of obstacles, using image sequences captured by video cameras mounted on the moving vehicle.

Many techniques of lane and obstacle detection are used in driver assistance systems. These techniques include the use of neural networks [1]; optical flow techniques [2]; identification of lane markings aided by color information and deformable templates [3]; model-based approaches [4]; re-organized image based approaches [5,6]; and so on.

Re-organized image based approaches use inverse perspective mapping (IPM) to remove perspective effect and reconstruct 3D road surface [7]. GOLD system [5] has been developed with a stereo vision-based hardware and software architecture. It includes three parts: detecting road markings through morphological processing, overcoming the annoying problems caused by non-uniform illumination, and implementing the detection step on massively parallel architectures in order to obtain real-time performance. It detects obstacles using stereo images. However, the system is quite vulnerable to road conditions. When the road is not flat (there is a slight slope in the road), the lane detection in GOLD cannot produce valid results.

RALPH system [6] decomposes the problem of lane

detection into three steps: (1) down-sampling of the input image to create a low resolution image, (2) determination of the road curvature in which a "hypothesize and test" strategy is employed, and (3) determination of the lateral offset of the vehicle relative to the lane center using a template-matching approach on the scan-line intensity profile generated in the curvature estimation step. However, it has two problems. One is that it has to adopt a strategy of down-sampling of the input image due to the large computational expense of obtaining the re-organized image, in which the resolution of the sampled image is too low to extract lane parameters effectively. The other problem is on a sloped road.

In this paper, a new approach to detection of a lane and obstacles is proposed, based on inverse-perspective mapping. In section 2, an improved inverse-perspective mapping is given, in order to improve the performance of the system. With IIPM, a re-organized image can be obtained quickly. Section 3 describes a new method of lane and obstacle detection from the re-organized image. Section 4 shows experimental results of lane state information obtained by the new method.

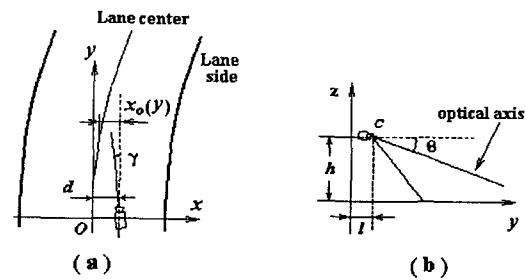


Fig. 1 Geometric model of camera system

2. IIPM for Recovery of 3D road surface

It is known that each pixel in 2D image plane represents a different area in the real world due to the perspective effect. The pixels near the bottom of the image plane correspond to smaller areas in the real world, while those pixels close to the top correspond to relatively larger areas and may possess more information about the road. Fig. 1 shows a geometric model of a lane, using one camera mounted in the vehicle. In the figure, (d, h, l) expresses the position of the camera in the real world. ω is the lane width, and γ and θ denote the vehicle deviation angle and inclination camera angle, respectively. Let $Oxyz$ and ouv denote 3D world space W

Detection using IIPM

A new method of detecting lane and obstacles based on IIPM is illustrated in Fig. 2. Lane parameters in the n -th frame input image consist of θ_n , γ_n , d_n , w_n , lane start location (x_{L0} and x_{R0}), lane curvature $1/R_n$, and of an existence of obstacles. When the system starts to detect lanes and obstacles, lane state parameters θ , γ , and d are first set as the initial camera parameters θ_0 , γ_0 , and d_0 , respectively. A gray-scale road image G_0 is once inputted, it is first transformed into the re-organized image G_1 by using Eq.(5). G_1 is filtered with two different one-dimensional filters, a weighted filter and a mean filter, and two resultant images are binarized, and the corresponding binary images G_2 and G_3 are obtained. G_2 and G_3 are separately processed with a size-filter and binary morphological filter, and the resultant images G_2 and G_3 are obtained. "AND" logic operation between G_2 and G_3 is performed, and the resultant image G_4 is used to detect the lane. Then, G_2 and the results of the lane detection are used to detect obstacles.

To determine the initial location of the lane, region identification technique is used to search the regions of lane marking in G_4 . According to the location of the searched lane markings on both sides of the right and left, the corresponding fitted-lines, L_L and L_R , are estimated as

$$L_L: \quad x = t_L y + x_{L0} \quad (6a)$$

$$L_R: \quad x = t_R y + x_{R0} \quad (6b)$$

where t_L and t_R express the reciprocals of the slopes of L_L and L_R , respectively. When the lane is approximately parallel to the vertical axis y of the re-organized image, t_L and t_R are very close to zero.

The central line between L_L and L_R , is easily obtained, and denoted by L_C . The upper part of G_4 is partitioned into four regions by L_L , L_R , and L_C , so that the left and right lane markings in the upper part of the re-organized image can be searched in these regions. To improve the reliability of the lane detection, the lane information of the previous frame of road image is used to check the fitted-lines L_L and L_R . Next, the lane state parameters are estimated. θ_n in the current road image is obtained by

$$\theta_n = \hat{\theta} + k_\theta \arccctg(t_R) - \arccctg(t_L) \quad (7)$$

where $\hat{\theta}$ is θ_0 or θ_{n-1} , $\theta(t_L, t_R) = \arccctg(t_R) - \arccctg(t_L)$, and

$$\theta_n = \theta_0 + \Delta\theta_n \quad (8)$$

where $\Delta\theta_n$ expresses the variance, produced by a sloped road surface or camera vibration.

The vehicle deviation angle γ_n is calculated by

$$\gamma_n = \hat{\gamma} + k_\gamma \gamma' \quad (9)$$

where $\hat{\gamma}$ is γ_0 or γ_{n-1} . k_γ is a constant, $\hat{\gamma} = \arccctg(t_C)$, t_C is the reciprocal of the slope of L_C . The lane width w_n equals to $\sin(\gamma')(x_{R0} - x_{L0})$, and the initial lane center offset d is equal to $d_0 + 0.5(x_{R0} - x_{L0})$.

After the lane is detected, G_2 and the detected lane information are used to determine whether there is any obstacle on the current lane or neighboring lanes. Fig. 4 illustrates the basic principle of obstacle detection in \mathcal{W} . Fig.4(a) shows an image G_0 in \mathcal{I} , in which there are three obstacles on the current lane and its two neighboring lanes. Fig.4(b) is the re-organized image in \mathcal{W} , obtained

and 2D image plane \mathcal{I} , respectively, where the original point O in \mathcal{W} is shown in Fig.1. According to semi-infinite pyramid view volume for perspective projection in computer graphics, the mapping between \mathcal{I} and \mathcal{W} is given by

$$u(x, y, 0) = k_u [\arctg(h \sin(\gamma_{xy}) / (x - d)) - (\theta - \alpha)] \quad (1)$$

$$v(x, y, 0) = k_v [\gamma_{xy} - (\gamma - \alpha)] \quad (2)$$

where k_u and k_v are coefficients of $k_u = 2\alpha / (M - 1)$ and $k_v = 2\alpha / (N - 1)$, and $\gamma_{xy} = \arctg(\frac{x-d}{y-l})$. 2α denote

the camera's angular aperture, and $M \times N$ is the camera resolution. In some system [5], the terms γ and θ in Eqs.(1) and (2) have been considered as constants, because it is assumed that road is flat, and there exist in precise road geometry. Although these assumptions can aid a lane detection algorithm and speed up the processing, they also result in low robustness and flexibility. In fact, γ and θ vary with time under real road conditions, which will require the hardware system to be quite complicated in order to improve the reliability and flexibility of the system. To solve the problem, a modified representation of Eq.(1), called IIPM, is given as follows

$$u(x, y, 0) = k_u [\arctg(h \sin(\gamma_{xy0}) / (x - d)) - (\theta_0 - \alpha)] - k_u \theta_\Delta \quad (3)$$

$$v(x, y, 0) = k_v [\gamma_{xy0} - (\gamma_0 - \alpha)] - k_v \gamma_\Delta \quad (4)$$

where $\gamma_{xy0} = \arctg(\frac{x-d_0}{y-l})$, $\theta = \theta_0 + \theta_\Delta$, $\gamma = \gamma_0 + \gamma_\Delta$. θ_0 and

γ_0 are the initial camera parameters, decided by the system, and they are all fixed. θ_Δ and γ_Δ are the differences between the initial values and the real camera parameters relative to the road surface. γ_{xy0} is also fixed for a given x and y , which implies that the first terms on the right side in Eqs.(3) and (4) are constants. So, Eqs.(3) and (4) are further represented by

$$u(x, y, 0) = u_0(x, y, 0) - k_u \theta_\Delta \quad (5a)$$

$$v(x, y, 0) = v_0(x, y, 0) - k_v \gamma_\Delta \quad (5b)$$

where $u_0(x, y, 0)$ and $v_0(x, y, 0)$ are fixed for given x and y .

Compared with Eqs.(3) and (4), the main advantage of Eq.(5) is to simplify the design of the hardware system without losing robustness and flexibility of the system. $u(x, y, 0)$ and $v(x, y, 0)$ can be exactly and obtained by Eq.(5) with very lower computational expense.

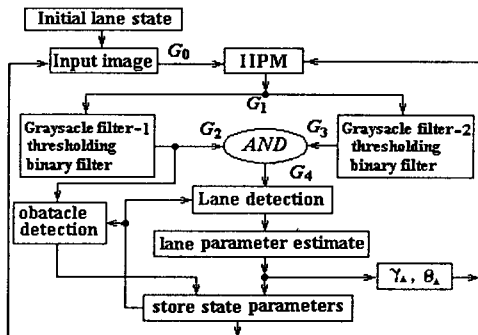


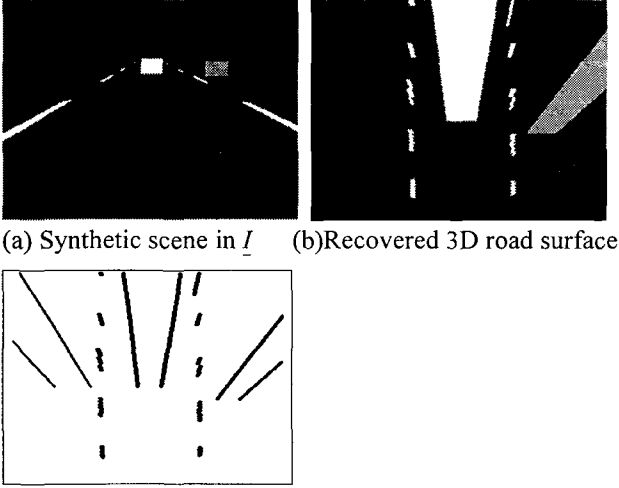
Fig. 2 A new method of lane state detection

3. New Approach of Lane and Obstacle

by IIPM. After some processing, G_2 is obtained and used to detect obstacles, in combination with the lane information. In Fig.4(c), the obstacle in each lane has its own feature, i.e., the specific directions of its straight-segments. The direction β of the straight segment is computed by

$$\beta = 0.5 \arctg\left(\frac{2\rho_{11}}{\rho_{20} - \rho_{20}}\right) \quad (10)$$

where ρ_{11} , ρ_{20} , and ρ_{02} denote the different central moments of the segment, respectively. The shape features of a segment in G_2 can be exploited to determine whether there is an obstacle in a given lane.



(a) Synthetic scene in I (b) Recovered 3D road surface
(c) Obstacle detection in G_2
Fig. 3 Analysis on detecting obstacle on 3D road surface

4. Experimental Results

An experimental system with one CCD camera sensor is established to test the proposed method. Figs.4(a) and (b) are a road image G_0 and the recovered road surface, G_1 , obtained by IIPM. Figs.4(c) and (d) show two processed binary images, G_2 and G_3 , and Fig. 4(e) is G_4 , $G_4 = G_2 \cap G_3$, which is used to detect the current lane. Region identification is operated to locate the lower parts of the lane markings. The fitted-lines, L_L and L_R , of these lane markings are estimated in Fig. 4(e), and their central-line L_C is also obtained. Three fitted-lines divide the upper half of the image into four parts, in which the upper parts of the lane markings are searched. Then, the lane parameters are estimated. The vehicle deviation angle γ_n is 0.57° , which implies that the lane tangent bends to the right. The radius of the lane curvature is about 1401.88m, the lane width is about 3.64m, and the lateral offset $x_0(y_0)$ in front of the vehicle 28m is about 0.25m. The detected lane structure and G_2 are used to determine if there are any obstacles on the current lane or neighboring lanes. From G_2 in Fig. 4(c), obstacles are detected, one in the current lane and the others in the left neighboring lane, according to the features in Fig.3(c).

Fig. 5(a) shows a test image, with a flat road surface, and Fig. 5(b) is estimated lines, l_R and l_L , in 2D image, here v_p is a vanishing point. Fig. 5(c) gives the mapping, L_R and L_L , of l_R and l_L in Fig. 5(b), obtained with θ . In Fig. 5(c), the dash lines represent the mapped results of

l_R and l_L with θ_c , which are parallel. L_R , L_L , and the vertical axis form two angles, γ_R and γ_L . When $\Delta\theta$ varies from -2° to 2° , the corresponding $\theta(t_L, t_R)$ is estimated and shown in Fig. 5(d). It is seen that there exists an approximately linear relation between $\theta(t_L, t_R)$ and $\Delta\theta$, in this case, $k_0 = 0.3129$. For Fig.5(c), $\Delta\theta$ is 0.50° , and γ_R and γ_L are computed as -1.2189° and 0.3657° . Based on γ_R and γ_L , $\Delta\theta$ is estimated as -0.4958° , which is quite close to its real value.

The new method may also be tested to detect lanes and obstacles in road images with a sloped road surface, in which the inclination camera angle θ has to be modified due to the slope. Fig. 6 shows one of performances. Using IPM with the initial inclination camera angle θ_0 , its re-organized image is obtained in Fig. 6(b). Figs. 6(c) and (d) are the corresponding G_2 and G_4 , obtained from Fig. 6(b). It is clear that L_L and L_R are not parallel because of the sloped road surface and the fixed θ_0 used, which results in some errors in detecting lane state. The sloped road surface calls for an increase in the real inclination camera angle, relative to the road surface, and it is not suitable to adopt the fixed inclination camera angle θ_0 . In this case, $\Delta\theta_n$ is estimated as 0.59° , it implies that the real inclination camera angle is 0.59° greater than θ_0 , and there is an up-sloped road surface. To overcome the problem, the new method uses variable inclination camera angle θ_c ($\theta_c = \theta_0 + \Delta\theta$), adaptively modified with L_L and L_R . Figs. 6(e) and (f) are G_2 and G_4 , obtained from the recovered road surface with θ_c . Compared with Fig. 6(c) and (d), more accurate estimate of lane state can be obtained from Figs. 6(e) and (f), which indicates that the new method has well robustness and flexibility.

Fig. 7 shows the results of parameter estimation in image sequence, where the horizontal axes denote the number of frame in image sequence. Fig. 7(a) is the estimated γ_n , which indicates the direction of the road. Fig. 7(b) is the estimated $\Delta\theta_n$, which shows that the inclination camera angle θ varies frequently because of the sloped road surface and vehicle vibration. Fig. 7(c) shows the lateral offsets $x_0(y_0)$ at 28m in front of the vehicle, which indicates the deviation of the vehicle from the lane center at the future 28m

5. Conclusions

Perspective effect makes pixels in the image plane have different meanings, depending on their position in the image. It leads to some difficulties in estimating the lane state parameters. IPM is often introduced to remove perspective effect, however, it also results in more complexity of the system. To reduce the computational expense of IPM, an IIPM is given in this paper so that the contradiction between the computation expense and the robustness of the system is alleviated. The proposed method of a lane and obstacle detection from a re-organized image uses some preprocessing techniques to enhance information on lane and obstacles. In the new algorithm, the inclination angle of camera can be adaptively calculated, which improves the accuracy of lane parameter estimation over that done with the fixed inclination camera angle. The test system uses only one

camera and then the complexity of the system is much reduced. Experimental results show that the system detects lane and obstacles well and gives an effective information on lanes to a driver assistant system.

References

[1] M. Rosenblum and L. S. Davis, "An Improved Radial Basis Function Network for Visual Autonomous Road Following," *IEEE Trans. on Neural Networks*, vol.7, p.1111-1120, 1996

[2] K. Kluge and S. Lakshmanan, "A Deformable Template Approach to Lane Detection," *Proc. IEEE Intelligent Vehicles '95*, Detroit, MI, p.54-59, 1995

[3] A. Broggi and S. Bertè, "Vision-Based Road Detection in Automotive Systems: a Real-Time Expectation-Driven Approach," *J. Artificial Intelligence Research*, vol.3, p.325-348, 1995

[4] J. D. Crisman and C. E. Thorpe, "SCARF: A Color Vision System That Tracks Roads and Intersections", *IEEE Trans. on Robot. Automat*, vol.9, p.49-58, 1993

[5] M. Bertozzi and A. Broggi, "GOLD: a Parallel Real-Time Stereo Vision System for Generic Obstacle and Lane Detection," *IEEE Trans on IP*, vol.7, p.62-81, 1998

[6] D. Pomerleau, "RALPH: Rapidly Adapting Lateral Position Handler," *Proc. IEEE Symposium on Intelligent Vehicles*, Detroit, USA, p.506-511, Sep. 1995

[7] Gang Yi Jiang, "Vision-Based Vehicle Guidance", *Ph. Dissertation*, Ajou University, Korea, 2000

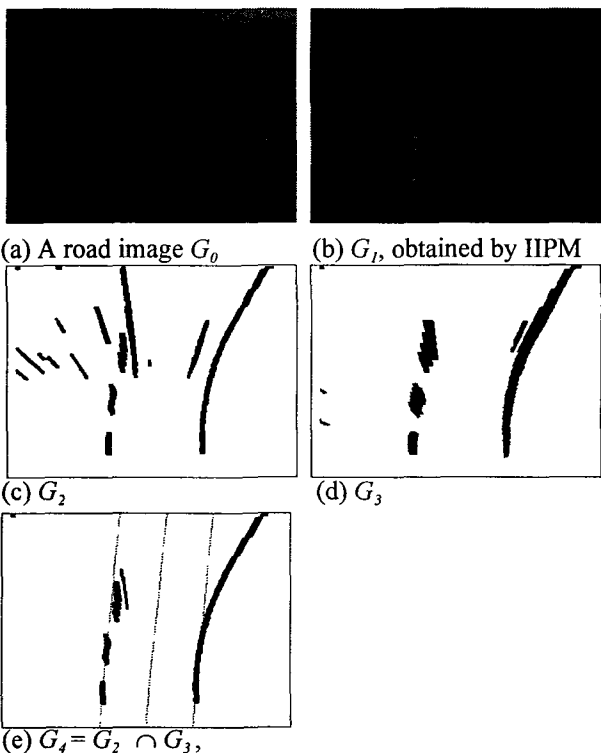


Fig. 4 Detect lane and obstacles using IIPM

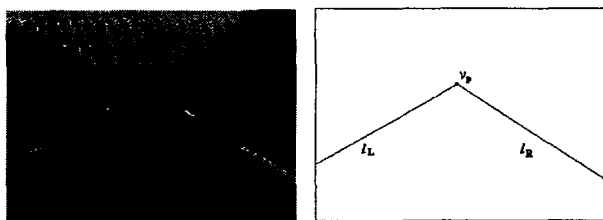


Fig. 5 Relationship between $\Delta\theta$ and $\theta(t_R, t_L)$

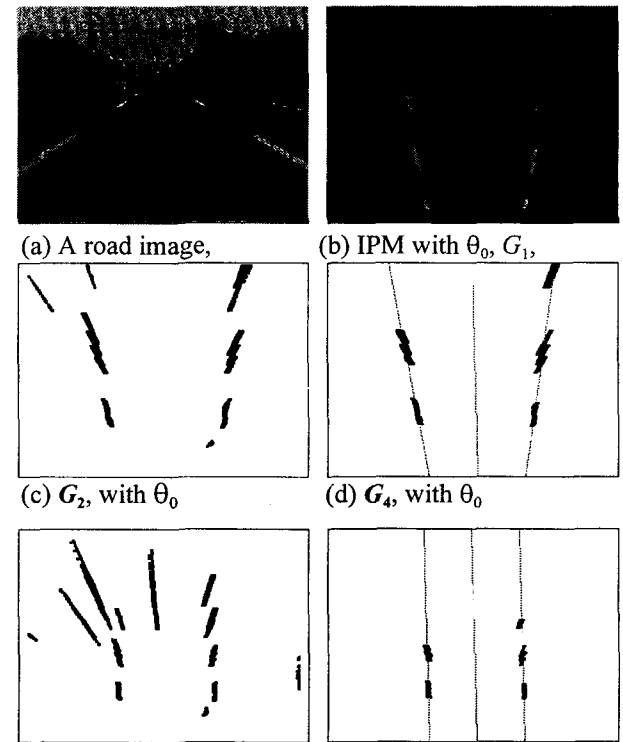
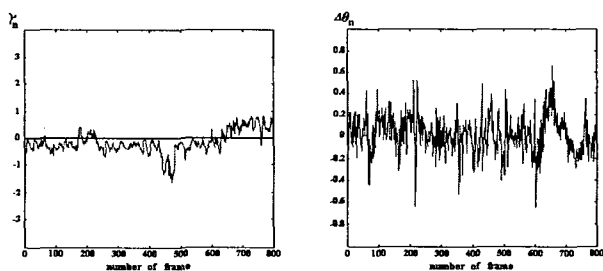


Fig. 6 Lane state detection with fixed θ_0 and adaptive θ_c . ($\theta_c = \theta_0 + \Delta\theta$)



(c) Lateral offset at 28m in front of the vehicle
Fig. 7 Lane parameters of image sequence